Dynamic Stokes Shift in Coumarin: Is It Only Relaxation?

Noam Agmon†

Physical Science Laboratory, DCRT, and Laboratory of Chemical Physics, NIDDK, National Institutes of Health, Bethesda, Maryland 20892 *(Received: July 31, 1989)*

Picosecond fluorescence spectra of coumarin 153 in solution show transient line narrowing. The peak's frequency shift and its area decay are nonexponential in time. A biexponential fit reveals a correlation between the fast exponents for the shift and area decay at different temperatures. A plot of shift as a function of area is temperature independent at short times. These findings are consistent with an inhomogeneous mechanism for the early part of the dynamic Stokes shift. Several suggested experiments may help distinguish between inhomogeneous and relaxation mechanisms.

1. Introduction

Dynamics of solvation is a rapidly growing field, as manifested by a number of recent review articles.[1,2] The simplest ultrafast solvation process occurs when a rigid dye molecule is electronically excited in a polar solvent. The excited molecule typically has a much larger dipole moment. When its fluorescence spectrum is followed as a function of time, a red shift is observed.[1-8] Initially, its peak is close to that of the absorption spectrum and with time approaches the maximum of the steady-state fluorescence spectrum. This "dynamic Stokes shift" has been first observed by Ware and co-workers[3] using nanosecond spectroscopy. Recent advances in laser technology enabled an extensive study of this phenomenon in the pico- and femtosecond time regimes.[4-8]

The above experimental findings have become the subject of growing theoretical interest.[9-15] A nearly universal underlying assumption in theoretical interpretation is that the transient spectral shift is due to relaxation of solvent molecules around the newly formed dipole. This point of view is undoubtedly influenced by an earlier idea of Onsager.[16] In spite of its pivotal role, this basic assumption has been neither challenged nor verified for dynamic solvation.

The above can be illustrated by the ubiquitous picture of two displaced parabolas for the ground- and excited-state potentials as a function of a "solvent coordinate" (Figure 1). Excitation is a "vertical" process, during which the solvent conformation has no time to change; hence, it produces conformations well displaced from the equilibrium conformation around the excited molecule. Since the vertical distance between the parabolas depends on the coordinate, the dye molecule fluoresces at a slightly different wavelength for different solvent conformations. Hence, the steady-state fluorescence spectrum is red-shifted (smaller energetic separation) compared to the excitation spectrum. The transient shift, it is argued, is due to solvent relaxation around the newly formed dipole which is mapped into the observed spectral relaxation.

In addition to shifting, it is observed that the spectral line narrows with time.[4-7] This has been interpreted[6] as an indication for a narrower solvation potential for the excited state, resulting from its larger dipole moment. The assumption that the shape of the potential along the solvation coordinate is mapped into the spectral line shape implies that this line shape must be, to some extent, inhomogeneously broadened. Hence, at every instant one observes a distribution of solvent conformations rather than a single conformation with a purely homogeneous line width. If this is so, the spectral shift may be due to the inhomogeneity in the spectrum in addition to solvent relaxation. This may occur if an excited molecule surrounded by solvent in conformations favorable for its ground state also converts faster to the ground state, as depicted by the arrows in Figure 1.

An inhomogeneous mechanism for chemical kinetics is well-documented for ligand binding to heme proteins.[17] In glasses at low temperatures it is known for over a decade that the observed kinetics reflect a distribution of barrier heights.[18] While a transient blue shift in the near-IR band of myoglobin following cryogenic ligand photodissociation has been initially attributed to protein relaxation,[19] it has subsequently been demonstrated[20-22] that, at least at very low temperatures, the shift is due to differential rebinding ("kinetic hole burning"[20]). The redder conformations, with the iron closer to the heme plane, also rebind faster and hence disappear first from the spectrum. As the temperature is increased, one expects a transition[23] from inhomogeneous kinetics of static conformations to dynamical relaxation.

It is not inconceivable that solvents at short times behave like glasses. The present paper therefore investigates the possibility that part of the dynamic Stokes shift is due to kinetic hole burning. Maroncelli and Fleming[6] have measured the transient picosecond fluorescence spectrum of a rigid dye molecule, coumarin 153, in 1-propanol at five different temperatures. Their data are suitable for analysis along the lines of ref 21. The analysis, described in detail below, shows that the shift at short times (over 50% of the

† Permanent address: Department of Physical Chemistry, The Hebrew University of Jerusalem, Jerusalem 91904, Israel.

(1) Kosower, E. M.; Huppert, D. *Annu. Rev. Phys. Chem.* **1986**, *37*, 127.
(2) (a) Simon, J. D. *Acc. Chem. Res.* **1988**, *21*, 128. (b) Barbara, P. F.; Jarzeba, W. *Ibid.* **1988**, *21*, 195. (c) Maroncelli, M.; MacInnis, J.; Fleming, G. R. *Science* **1989**, *243*, 1674.
(3) (a) Ware, W. R.; Chow, P.; Lee, S. K. *Chem. Phys. Lett.* **1968**, *2*, 356. (b) Ware, W. R.; Lee, S. K.; Brant, G. J.; Chow, P. P. *J. Chem. Phys.* **1971**, *54*, 4729. (c) Chakrabati, S. K.; Ware, W. R. *Ibid.* **1971**, *55*, 5494.
(4) (a) Nagarajan, V.; Brearley, A. M.; Kang, T. J.; Barbara, P. F. *J. Chem. Phys.* **1987**, *86*, 3183. (b) Kahlow, M. A.; Kang, T. J.; Barbara, P. F. *Ibid.* **1988**, *88*, 2372. (c) Jarzeba, W.; Walker, G. C.; Johnson, A. E.; Kahlow, M. A.; Barbara, P. F. *J. Phys. Chem.* **1988**, *92*, 7039. (d) Kahlow, M. A.; Jarzęba, W.; Kang, T. J.; Barbara, P. F. *J. Chem. Phys.* **1989**, *90*, 151.
(5) Castner, Jr., E. W.; Maroncelli, M.; Fleming, G. R. *J. Chem. Phys.* **1987**, *86*, 1090.
(6) Maroncelli, M.; Fleming, G. R. *J. Chem. Phys.* **1987**, *86*, 6221.
(7) (a) Su, S.-G.; Simon, J. D. *J. Phys. Chem.* **1986**, *90*, 6457; **1987**, *91*, 2693. (b) *J. Chem. Phys.* **1987**, *87*, 7016.
(8) Declémy, A.; Rullière, C. *Chem. Phys. Lett.* **1988**, *145*, 262; **1988**, *146*, 1.
(9) (a) Bagchi, B.; Oxtoby, D. W.; Fleming, G. R. *Chem. Phys.* **1984**, *86*, 257. (b) Bagchi, B.; Chandra, A. *J. Chem. Phys.* **1989**, *90*, 7338.
(10) van der Zwan, G.; Hynes, J. T. *J. Phys. Chem.* **1985**, *89*, 4181.
(11) Sumi, H.; Marcus, R. A. *J. Chem. Phys.* **1986**, *84*, 4272, 4894. Nadler, W.; Marcus, R. A. *Ibid.* **1987**, *86*, 3906.
(12) Wolynes, P. G. *J. Chem. Phys.* **1987**, *86*, 5133.
(13) (a) Rips, I.; Jortner, J. *J. Chem. Phys.* **1987**, *87*, 2090, 6513. (b) Rips, I.; Klafter, J.; Jortner, J. *Ibid.* **1988**, *88*, 3246; **1988**, *89*, 4288.
(14) Loring, R. F.; Yan, Y. Y.; Mukamel, S. *Chem. Phys. Lett.* **1987**, *135*, 23; *J. Phys. Chem.* **1987**, *91*, 1302.
(15) Maroncelli, M.; Fleming, G. R. *J. Chem. Phys.* **1988**, *89*, 875, 5044.
(16) Onsager, L. *Can. J. Chem.* **1977**, *55*, 1819.
(17) Frauenfelder, H.; Wolynes, P. G. *Science* **1985**, *229*, 337.
(18) (a) Austin, R. H.; Beeson, K. W.; Eisenstein, L.; Frauenfelder, H.; Gunsalus, I. C. *Biochemistry* **1975**, *14*, 5355. (b) Ansari, A.; Berendzen, J.; Braunstein, D.; Cowen, B. R.; Frauenfelder, H.; Hong, M. K.; Iben, I. E. T.; Johnson, J. B.; Ormos, P.; Sauke, T. B.; Scholl, R.; Schulte, A.; Steinbach, P. J.; Vittitow, J.; Young, R. D. *Biophys. Chem.* **1987**, *26*, 337.
(19) Ansari, A.; Berendzen, J.; Bowne, S. F.; Frauenfelder, H.; Iben, I. E. T.; Sauke, T. B.; Shyamsunder, E.; Young, R. D. *Proc. Natl. Acad. Sci. U.S.A.* **1985**, *82*, 5000.
(20) Campbell, B. F.; Chance, M. R.; Friedman, J. M. *Science* **1987**, *238*, 373.
(21) Agmon, N. *Biochemistry* **1988**, *27*, 3507.
(22) Ansari, A. Ph.D. Thesis, University of Illinois, Urbana, IL, 1988.
(23) (a) Agmon, N.; Hopfield, J. J. *J. Chem. Phys.* **1983**, *78*, 6947. (b) *Ibid.* **1983**, *79*, 2042.

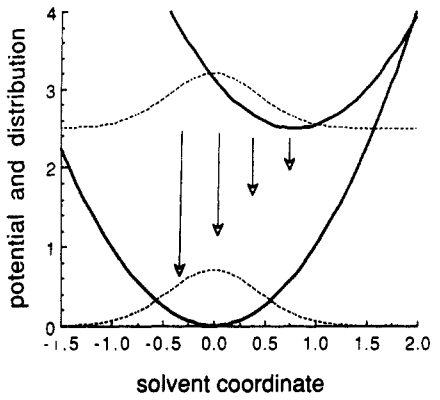

Figure 1. Schematic representation of Stokes shift dynamics. Full, bold curves represent ground and excited potential energy surfaces as a function of a solvent coordinate. An initial distribution of solvent conformations (lower dashed curve) is unaltered upon electronic excitation (upper dashed curve). This distribution could subsequently move to the right either by relaxation toward the bottom of the excited-state well or due to a coordinate-dependent decay rate, as depicted by the arrows.

total shift) is indeed consistent with an inhomogeneous mechanism. A series of suggested experiments could assess the extent of this effect on the observed time-dependent Stokes shifts.

2. Theory

Although more elaborate theories are available,[23] it is instructive to illustrate the differences between the relaxation and imhomogeneous mechanisms discussed in the introduction with the aid of a simple kinetic model. This model is not expected to fit any of the data quantitatively but would exemplify the qualitative correlations on which we base the analysis of experimental results in the next section.

We begin by postulating two "solvent conformations", A and B, each with a rectangularly shaped spectral line of full width 1/2 (in some arbitrary frequency scale denoted by x) and an initial height of unity. For sake of demonstration, we assume that the two conformations have equal extinction coefficients and initial probabilities. Hence, at $t = 0$ the two half-peaks are equal in amplitude, so the observed intensity is

$$I(x,0) = 1, \quad 0 \le x \le 1$$
$$I(x,0) = 0, \quad x < 0, 1 < x \tag{1}$$

This is demonstrated in Figure 2. The total area of $I(x,0)$, denoted below by $a(t)$, is unity, and its average frequency is $\bar{x}(0) = 1/2$. As the intensities of the two half-lines change according to kinetic schemes below, $a(t)$ diminishes and $\bar{x}(t)$ shifts. While each of the half-lines is assumed to have a constant width of 1/2 at all times, the width of the combined line at the height corresponding to $a(t)/2$ could change discontinuously from 1 to 1/2. In this section we focus attention on the implied relationship between shift and area.

The two simple schemes below were chosen to mimic relaxation and inhomogeneous kinetics. In both models, A and B are assumed to decay with a rate constant k_0, k_0^{-1} being the analogue of a radiative lifetime. In addition, we assume a second rate process, with a rate coefficient k, which has different roles in the two models. In the relaxation model

$$\begin{array}{ccc} A & \xrightarrow{k} & B \\ \downarrow k_0 & & \downarrow k_0 \end{array} \tag{2}$$

k is the rate coefficient for transitions from A to B. In the inhomogeneous scheme

$$\begin{array}{cc} A & B \\ \downarrow k_0+k & \downarrow k_0 \end{array} \tag{3}$$

there are no transitions between A and B, but the decay of A is faster than that of B due to an additional decay process, say, nonradiative decay, represented by the rate constant k.

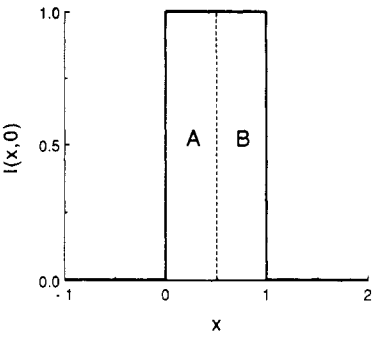

Figure 2. A simple model for a fluorescence line shape which is both inhomogeneously and homogeneously broadened. x is frequency or wavelength in some arbitrary units. The inhomogeneous broadening is due to the existence of two solvent conformations, A and B, which emit at $x = 1/4$ and 3/4. Each of the two bands is homogeneously broadened, with a homogeneous full width of 1/2 and identical intensities.

It is easy to evaluate the time dependence of the area, $a(t)$, and average frequency, $\bar{x}(t)$, for the two models assuming equal initial probabilities for A and B. For the relaxation model (2), we obtain

$$a(t) = \exp(-k_0 t) \tag{4a}$$
$$\bar{x}(t) = \tfrac{1}{8}\exp(-kt) + \tfrac{3}{8}[2 - \exp(-kt)] \tag{4b}$$

In eq 4b, the factors 1/4 and 3/4 are the mean frequencies of the two half-lines and the weights with respect to which the average is calculated are the areas of the half-bands divided by the total area, $a(t)$. Therefore, the factor $\exp(-k_0 t)$ does not appear. The exponential terms come from the solution of the rate equations for scheme 2. Likewise, for the inhomogeneous scheme 3 we find that

$$a(t) = \tfrac{1}{2}\exp(-k_0 t)[1 + \exp(-kt)] \tag{5a}$$
$$\bar{x}(t) = \tfrac{1}{4}[3 + \exp(-kt)]/[1 + \exp(-kt)] \tag{5b}$$

In both cases $a(t)$ decays from unity to zero and $\bar{x}(t)$ shifts from 1/2 to 3/4.

The qualitative difference between eqs 4 and 5 is evident: For the relaxation model, eq 4, there is no relation between area and shift, as only the latter depends on the rate constant k. In contrast, the inhomogeneous mechanism, eq 5, implies that both area and shift have an identical fast decay component, $\exp(-kt)$. When spectral shift is fast compared to radiative lifetime, $k \gg k_0$, then for $k_0 t \ll 1$ we may replace $\exp(-k_0 t)$ by 1. Under these conditions the observed shift becomes a simple function of the area

$$\bar{x}(t) = \tfrac{1}{4}[1 + a(t)^{-1}] \tag{6}$$

As $a(t)$ decreases from 1 to 1/2 due to the disappearance of the peak corresponding to state A from the spectrum, the overall mean frequency shifts from 1/2 to 3/4. In a situation where k varies say, with temperature, eq 6 predicts a universal relation between shift and area irrespective of temperature.

While the specific model above is oversimplified, only the quantitative aspects of eq 6 depend on details such as line shapes, number of conformations, etc. The mere existence of a correlation between shift and area follows from the basic property of an inhomogeneous broadening mechanism in which different conformations both fluoresce at different wavelengths and react with different rates.

3. Results

The results reported in this section are based on the picosecond measurements by Maroncelli and Fleming[6] of the dynamic Stokes shift of coumarin 153 in 1-propanol in the temperature range 222–298 K. In ref 6, the decay of the fluorescence intensity as a function of time at various wavelengths, $I_\lambda(t)$, was deconvoluted from the instrument response function (110-ps fwhm) and fit to a sum of 1–3 exponentials. To obtain the spectrum as a function of wavelength at different times, $I_t(\lambda)$, one may invoke the property that the steady-state (SS, continuous illumination) fluorescence

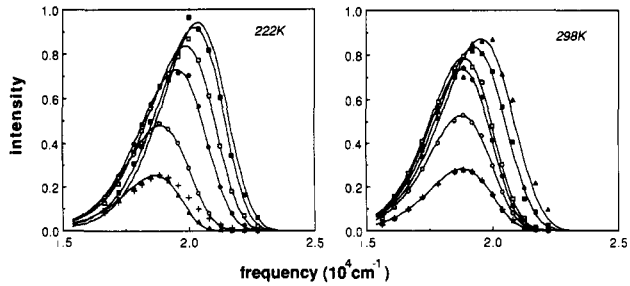

Figure 3. Transient fluorescence spectra of coumarin 153 in 1-propanol at the two most extreme temperatures monitored in ref 6. Points are experimental data, rearranged according to eq 7, at t = 20 (open triangles), 50 (full squares), 200 (open squares), 500 (full circles), 2000 (open circles), and 5000 ps (full triangles). Plus signs represent the steady-state spectrum rescaled to the transient data at 5 ns. Lines are best fit to a log-normal distribution, eq 8.

spectrum, $I_{SS}(\lambda)$, is the time integral of the transient spectra, $I_t(\lambda)$. This gives

$$I_t(\lambda) = I_\lambda(t)\, I_{SS}(\lambda) / \int_0^\infty I_\lambda(t)\, dt \qquad (7)$$

Evidently, the accuracy of the procedure depends on accurate knowledge of both SS spectrum and time integral of the kinetic traces. Since the short-time fluorescence spectrum is shifted to the blue relative to the SS spectrum, its blue edge is least accurately determined by the above procedure. The performance of the time integral introduces additional inaccuracies due to the unresolved short-time behavior of $I_\lambda(t)$ and its unmeasured long-time dependence. The latter was corrected for by assuming that the experimental traces, followed in ref 6 up to 5 ns, can be extrapolated to 10 ns from the multiexponential fits and to longer times using the overall fluorescence lifetime as determined by nanosecond fluorescence measurements.

The spectra, measured at typically 10–15 wavelengths, are fitted to a log-normal distribution[24,25]

$$I_t(\nu) = \frac{I_0}{1 + \beta\Delta\nu} \exp[-\alpha \ln^2 (1 + \beta\Delta\nu)] \qquad (8)$$

where $\Delta\nu \equiv \nu_p - \nu$ and $\nu \equiv 1/\lambda$ in units of cm^{-1}. There are four free parameters in the fit: The amplitude at the peak, I_0, the width/skewdness parameters, α and β, and the frequency at the peak, ν_p. The log-normal distribution is a skewed Gaussian distribution. (It tends to a Gaussian as $\beta\Delta\nu \to 0$.) Since it is obtained from a Gaussian distribution by a simple change of variables, its area, a, and full width at half-height, w, are given by

$$a = I_0[\pi/(\alpha\beta^2)]^{1/2} \qquad (9)$$

$$w = [\exp(\Delta) - \exp(-\Delta)]/[\beta \exp(2\alpha)^{-1}]$$

$$\Delta^2 \equiv (2\alpha)^{-2} + (\ln 2)/\alpha \qquad (10)$$

To exact the four parameters, we have used a nonlinear least-squares routine, utilizing a mixed gradient/Hessian algorithm together with the analytical first (and, optional, second) derivatives of $I_t(\nu)$, eq 8, with respect to the parameters.[26]

The spectra obtained by this procedure for the two extreme temperatures at different times are shown in Figure 3. The symbols represent the experimental data, rearranged according to eq 7, while the full lines are the best fits to the log-normal distribution, eq 8. The SS spectrum (normalized to the amplitude of the longest time spectrum) is shown as plus signs. At 298 K the shift occurs extremely fast and the transient spectrum converges to the SS spectrum. In contrast, at 222 K the spectrum at long times is red-shifted relative to the SS spectrum. This is due to a slower transient shift which results in some contribution of the early time spectra to the time integral defining I_{SS}. Evidently, the fit to eq 8 is not as good for short times (two of which are within the instrument response function) as at longer times. One notes from Figure 3 that, when the amplitude is not renormalized, the depletion of the blue edge becomes a significant part of the overall shift.

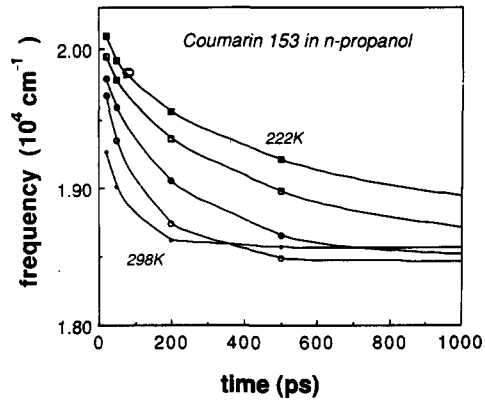

Figure 4. Transient shift of the frequency of the peak, ν_p, as determined from fitting eq 8 to data such as shown in Figure 3. The five temperatures are[6] (top to bottom) 222, 233, 253, 273, and 298 K.

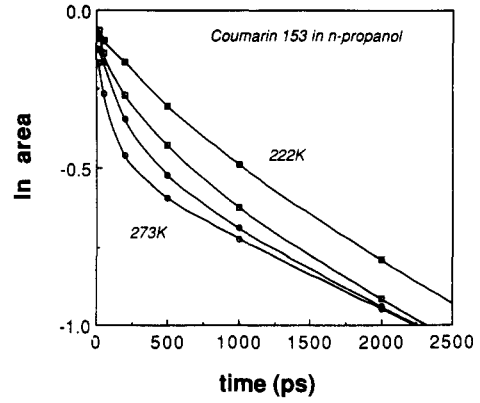

Figure 5. Transient decay of the area of the fluorescence peak, $a(t)$, as calculated in eq 9 from the best-fit parameters of eq 8. Temperatures as in Figure 4, excluding 298 K.

The transient shift in the peak frequency, ν_p, at five temperatures is plotted against time in Figure 4. A plot of the average frequency, $\bar{\nu}$, looks qualitatively similar (see Figure 11a in ref 6). The accuracy in determining the shift tends to decrease with increasing temperature: The data at 298 K are most inaccurate, as the shift occurs largely within the instrument response function. At the lower temperatures the experimental time resolution is adequate. While improved time resolution can help in determining whether the "t = 0" origin is temperature independent, at longer times the shift is clearly strongly temperature dependent, the higher the temperature the faster the shift. The functional form of the fit is not monoexponential: It could be fit to either a sum of exponentials or a stretched exponential.[6]

Figure 5 shows the transient decrease in the peak's area, eq 9. It is similarly multiexponential and temperature dependent. Only at long times the curves approach a single, temperature-independent, exponential decay. The curves in Figure 5 have been fitted to a biexponential. The longer of the two time constants obtained is 4.5 ± 0.3 ns and, within these error bars, is temperature independent. This number agrees with the radiative lifetime obtained by nanosecond measurements (see Table III in ref 6). The smaller of the two time constants contributes about 30% to the t = 0 amplitude and is strongly temperature dependent.

The faster of the two decay times of the average frequency (τ_2 in Table V, ref 6) is plotted in Figure 6 against the faster decay time of the integrated intensity for the various temperatures studied. The two decay times are clearly correlated. The straight line in figure 6 has a slope of 0.7 and intercept of −12 ps. While

(24) Stuart, A.; Ord, K. J. *Kendall's Advanced Theory of Statistics*, 5th ed.; Oxford University Press: New York, 1987; Vol. 1.
(25) Siano, D. B.; Metzler, D. E. *J. Chem. Phys.* **1969**, *51*, 1856.
(26) Kaniel, S.; Dax, A. *SIAM J. Numer. Anal. 179*, 16, 324.

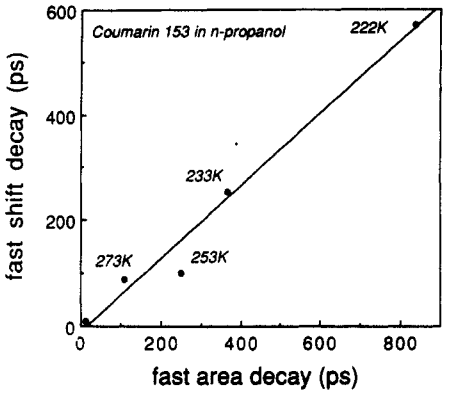

Figure 6. The faster of the two decay times for $\bar{\nu}$ (τ_2 in Table V of ref 6) vs the faster of the two decay times for $a(t)$, as obtained from a biexponential fit to the data in Figure 5. The different temperatures (except 298 K) are indicated on the plot. Full curve is a linear fit with an intercept of −12 ps and a slope of 0.69.

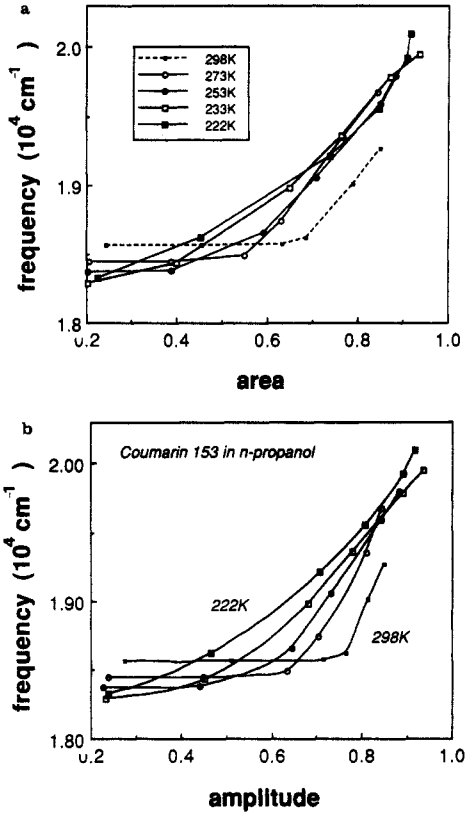

Figure 7. (a) Peak frequency, ν_p, vs area, $a(t)$, for the five temperatures indicated in the legend. Lines are interpolations. (b) Same as (a) except as a function of the peak's amplitude, I_0.

this intercept is zero to within experimental accuracy, the slope deviates from the value of unity suggested for an inhomogeneous mechanism by the simple model of section 2. It is nevertheless much closer to 1 than to the value 0 expected for a relaxation mechanism.

As a second test,[21,22] Figure 7a shows the shift in ν_p as a function of $a(t)$. As suggested by eq 6, a universal correlation between peak frequency and area is observed at early times, namely, when $a(t)$ is close to 1. The curves for all temperatures (except 298 K) fall on the same line at least down to $a(t) = 0.75$. This corresponds to times up to 500 ps at 222 K and 200 ps at 273 K. During this initial period over 50% of the shift has occurred. The data at 298 K deviates perhaps because at that temperature the shift is faster than the experimental time resolution. As seen in Figure 7b, a similar behavior is observed when the shift is plotted against the amplitude, I_0. This plot may involve somewhat smaller errors, because I_0 is one of the fitting parameters while $a(t)$ is a combination of three of the fitting parameters; see eq 9.

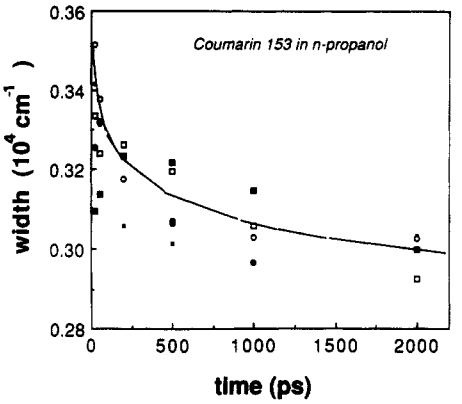

Figure 8. Width, $w(t)$, as calculated using eq 10 and the best-fit parameters to eq 8, as a function of time. Temperatures are as in the legend of Figure 7a, and the line is merely to guide the eye.

Finally, Figure 8 shows the width, eq 10, as a function of time. The symbols are the data at different temperatures. At long times the width is generally larger at higher temperatures. For all temperatures it is clear that the bandwidth decreases with time. Since it is more difficult to determine the width than it is to determine the peak's amplitude and frequency, we have drawn a curve simply to guide the eye.

4. Discussion

This paper has analyzed the transient Stokes shift observed[6] for a rigid dye molecule. The initial width of the fluorescence spectrum decreases with time. While this can be interpreted as either a narrower excited-state potential or a faster decay of the blue edge, both interpretations imply that there must be some degree of inhomogeneous line broadening. The correlation between the fast decay times of the area and the shift at different temperatures and the equivalent statement that a plot of shift vs area shows universal, T-independent behavior at short times are both consistent with an inhomogeneous interpretation for the short-time behavior. In this interpretation the excited molecule surrounded by solvent in conformations commensurate with its ground-state decays to it faster. Since these conformations are blue-shifted, and the line shape is partially inhomogeneously broadened, the spectrum shifts to the red.

The detection of inhomogeneous effects is complicated by solvent relaxation, which becomes dominant at long times. Therefore, additional suggested experiments may help in differentiating between the mechanisms responsible for the shift:

Absolute Quantum Yields. The relative insensitivity of the radiative lifetime to temperature compared to the large variation in the rate of frequency shift with T suggests that if an inhomogeneous mechanism is indeed causing some of the shift, this mechanism is nonradiative. Accurate measurements of the absolute quantum yield (ratio of photon absorbed to photons emitted), especially at short times, could determine whether a nonradiative fluorescence quenching pathway plays a role in the decay of the coumarin fluorescence.

Low-Temperature Experiments. One may argue that in glasses no solvent relaxation is anticipated. An older nanosecond measurement[3c] below the freezing point of 1-propanol and a recent picosecond measurement[27] (time scale 100 ps-10 ns) on a different coumarin molecule in a butanediol glass at 88 K show a definite though small shift. It would be interesting to follow the kinetics in glasses to much longer times by using either sensitive time-correlated single-photon counting or probe molecules with longer radiative lifetimes. For an inhomogeneous mechanism one expects, in analogy to heme protein kinetics,[17,23] a multiexponential shift on a slower time scale.

Temperature Cycling. This suggestion is modeled after an experiment designed to demonstrate kinetic hole burning in myoglobin.[20] The sample is first cooled to near 0 K and the

(27) Maroncelli, M. Unpublished data.

fluorescence spectrum recorded. This serves as a reference, unrelaxed spectrum. Next an intense light source is applied, so that 100% of the dye molecules are excited. The sample is heated to an appropriate temperature under illumination and cooled down again to near 0 K. Finally, the intense light source is turned off and the fluorescence spectrum recorded again. If relaxation has taken place at the elevated temperature, the spectrum measured after recooling should be shifted accordingly.

Pulse-Train ("Pumping") Experiment. This suggested experiment is also modeled after a heme protein experiment.[18b] Suppose the sample is irradiated by an intense laser emitting a pulse train with a repetition rate that is high compared to the average Stokes shift duration (e.g., a 50-ps pulse emitted every 500 ps for a coumarin sample at 220 K). The transient fluorescence spectra are measured as a function of a pulse-train duration after the last pulse in the train. If a relaxation mechanism operates, we expect that each pulse in the train promotes partial relaxation of the solvent toward its excited-state configuration. Between pulses, the solvent does not completely relax in the opposite direction before an additional pulse in the train promotes additional relaxation. The expected effect is of larger relaxation for longer pulse-train duration.

Gas-Phase Measurements. The line shape and decay kinetics in the gas phase should be measured and used as a reference for the solution-phase measurements.[28]

Optical Hole Burning. If the line shape is inhomogeneously broadened, it should be possible to burn a hole in the absorption spectrum by using a narrow excitation band.[29] Such measurements could determine the relative magnitude of inhomogeneous vs homogeneous line broadening.[30] In addition, fluorescence decay could be monitored as a function of excitation wavelength. In the limit that only a single conformation is excited, the inhomogeneity is removed and the only mechanism for shift is relaxation.

Acknowledgment. I am grateful to Mark Maroncelli and Graham R. Fleming for permission to use the data of ref 6. I thank Mark Maroncelli for suggesting the presentation in Figure 6 and Attila Szabo for suggestions of appropriate kinetic schemes. This work was supported in part by USA-Israel Binational Science Foundation Grant 86-00197.

Registry No. Coumarin 153, 53518-18-6.

(28) Ernsting, N. P.; Asimov, M.; Schäfer, F. P. *Chem. Phys. Lett.* **1981**, *91*, 231.
(29) Hayes, J. M.; Jankowiak, R.; Small, G. J. In *Persistent Spectral Hole Burning: Science and Application*; Moerner, W. E., Ed.; Springer: New York, 1987. Friedrich, J.; Haarer, D. *Angew. Chem., Int. Ed. Engl.* **1984**, *23*, 113.
(30) Ormos, P.; Ansari, A.; Braunstein, D.; Cowen, B. R.; Frauenfelder, H.; Hong, M. K.; Iben, I. E. T.; Sauke, T. B.; Steinbach, P.; Young, R. D. *Biophys. J.*, in press.

The 248-nm Photofragmentation of the CH_3O_2 Radical

D. Hartmann, J. Karthäuser,

Institut für Physikalische Chemie, Universität Göttingen, D-3400 Göttingen, FRG

and R. Zellner*

Institut für Physikalische Chemie und Elektrochemie, Universität Hannover, D-3000 Hannover, FRG
(Received: August 4, 1989; In Final Form: November 9, 1989)

The products of the photodissociation of CH_3O_2 in the 248-nm (KrF) excimer laser photolysis have been investigated by using both emission spectroscopy and laser-induced fluorescence (LIF). Among the products $OH(A^2\Sigma^+)$, $OH(X^2\Pi)$, and $CH_3O(\tilde{X}^2E)$ have been identified with fractional yields of the latter two of $\varphi(OH) = 0.06 \pm 0.03$ and $\varphi(CH_3O) = 0.2 \pm 0.1$. Formation of $OH(A^2\Sigma^+)$ is suggested as a diabatic process involving an excited state of CH_2OOH. The observed emission is sufficiently strong to utilize the 248-nm photodissociation of CH_3O_2 as a monitor of this species in kinetic experiments.

Introduction

The CH_3O_2 radical has a well-known near-UV absorption with an absorption coefficient at maximum near 235 nm of $\sigma = (4.8 \pm 0.4) \times 10^{-18}$ cm^2.[1-3] The corresponding electronic transition has not been fully characterized but based on the analogy with HO_2 probably corresponds to $\tilde{X}^2A'' - \tilde{B}^2A''$ which is both spin and orbital allowed. The structure of the spectrum suggests that the excited CH_3O_2 state is predissociative with the energetically possible fragmentation channels (with ΔH_R/kJ mol^{-1} values in parentheses) given in Scheme I. As a consequence we may expect cleavage of the O-O bond as well as of the (weaker) C-O bond. The most exothermic products are $CH_2O + OH$ which may be formed by O-O bond cleavage from CH_2OOH after initial isomerization of CH_3O_2. Among the electronically excited fragments O_2(X,a,b), $OH(A^2\Sigma^+)$ and $CH_2O(\tilde{A}^1A'')$ are energetically possible. Formation of excited $CH_3O(\tilde{A}^2A_1)$ and $CH_3(\tilde{A}^2A'')$ is endothermic by 143 and 553 kJ mol^{-1}, respectively, and can therefore not be obtained with 248-nm radiation in a one-photon process.

Investigations of the photodissociation products of CH_3O_2 have to our knowledge not been performed previously. One of the interesting questions is whether the photodissociation of CH_3O_2,

SCHEME I

$$CH_3O_2 + h\nu(248\text{ nm}) \rightarrow CH_3O(\tilde{X}^2E) + O(^3P) \quad (-234.0)$$
$$\rightarrow CH_3O(\tilde{X}^2E) + O(^1D) \quad (-44.3)$$
$$\rightarrow CH_3(\tilde{X}^2A_2'') + O_2(X^1\Sigma_g) \quad (-353.0)$$
$$\rightarrow CH_3(\tilde{X}^2A_2'') + O_2(a^1\Delta_g) \quad (-258.7)$$
$$\rightarrow CH_3(\tilde{X}^2A_2'') + O_2(b^1\Sigma_g) \quad (-196.1)$$
$$\rightarrow CH_2O(\tilde{X}^1A_1) + OH(X^2\Pi) \quad (-569.5)$$
$$\rightarrow CH_2O(\tilde{X}^1A_1) + OH(A^2\Sigma^+) \quad (-183.1)$$
$$\rightarrow CH_2O(\tilde{A}^1A'') + OH(X^2\Pi) \quad (-239.5)$$

* Author to whom correspondence should be addressed.

(1) Jenkin, M. A.; Cox, R. A.; Hayman, G.; Whyte, L. J. *J. Chem. Soc. Faraday Trans. 2* **1988**, *84*, 913.
(2) Simon, F.; Schneider, W.; Moortgat, G. *Int. J. Chem. Kinet.*, in press.
(3) Moortgat, G.; Veyret, R.; Lesclaux, R *J. Phys. Chem.* **1989**, *93*, 2368.

0022-3654/90/2094-2963$02.50/0